Int. J. Heat Mass Transfer Vol. 33, No. 9, pp. 1921–1928, 1990
Printed in Great Britain

0017-9310/90 $3.00 + 0.00

Prediction of critical heat flux of subcooled flow boiling in round tubes

Y. KATTO
Department of Mechanical Engineering, Nihon University, Kanda-Surugadai, Chiyoda-ku, Tokyo 101, Japan

(*Received* 4 *July* 1989)

Abstract—Based on the liquid sublayer dryout mechanism, a physical model of critical heat flux (CHF) of subcooled flow boiling is presented in a previous paper with a rather tentative correlation of a coefficient k to link the velocity of a vapor blanket with that of two-phase flow. In the present paper, a new correlation of the velocity coefficient k is derived based on CHF data of various kinds of fluids, presenting a generalized method to predict CHF of subcooled flow boiling within the range of subcooling $T_{sat} - T_L \geq 0$ K, void fraction $x < 0.7$, and vapor/liquid density ratio $\rho_v/\rho_L > 0.01$. Comparisons of predicted and measured CHF show fairly good accuracy up to high degrees of subcooling.

1. INTRODUCTION

As for critical heat flux (CHF) of subcooled flow boiling, the first analysis based on the liquid sublayer dryout mechanism was presented by Lee and Mudawar [1], showing good accuracy to predict the CHF of water up to rather high degrees of subcooling.

Then, following the same principle as above, a somewhat different type of analysis was presented by the author [2], offering a predictive procedure of CHF which is summarized in the Appendix. This analysis postulates a flow structure such as that illustrated schematically in Fig. 1, where CHF is assumed to occur when a liquid sublayer of initial thickness δ is dried out due to evaporation during the passage time of a vapor blanket of length L_B and velocity U_B sliding on the liquid sublayer. In order to evaluate the sublayer thickness δ, a dimensionless correlation of δ derived in a previous study of CHF in pool boiling [3] is applied, while the vapor blanket velocity U_B is evaluated by relating it to the local velocity U_o of the two-phase flow (which is assumed to be homogeneous flow) at the distance of δ from the tube wall as follows:

$$U_B = kU_o. \tag{1}$$

The velocity coefficient k on the right-hand side of equation (1) is only one quantity to be determined empirically in this model. In the previous paper [2], CHF data of subcooled flow boiling of water in an 8 mm diameter tube, included in the CHF table of the U.S.S.R. Academy of Sciences [4], were analyzed to give the following dimensionless correlation of k:

for $x = 0.25$–0.7

$$k = \frac{6.4 \times 10^3}{1 + 87.3(\rho_v/\rho_L)^{1.28}} Re^{-0.8}$$

for $x = 0$–0.25

$$k = \frac{1.5 \times 10^4}{1 + 87.2(\rho_v/\rho_L)^{1.19}} Re^{-0.8}$$

for $x = 0$

$$k = \frac{6 \times 10^3}{1 + 254(\rho_v/\rho_L)^{2.83}} Re^{-0.8} \tag{2}$$

where x is the void fraction, ρ_v/ρ_L the vapor liquid density ratio, and Re the Reynolds number. Also, it has been found that the foregoing predictive procedure employing k of equation (2) is applicable to predict CHF not only for water including various tube diameters other than 8 mm, but also for non-aqueous

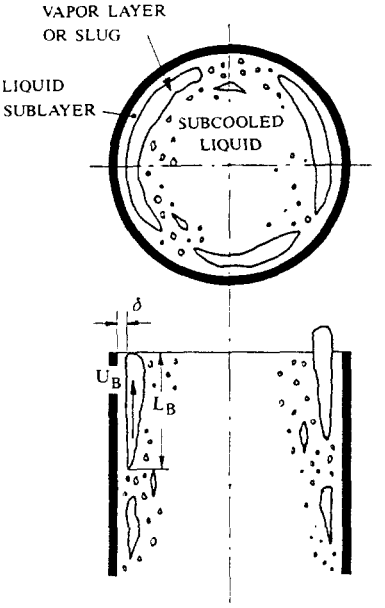

FIG. 1. Subcooled flow boiling near CHF conditions.

NOMENCLATURE

c_{pL}	specific heat of liquid at constant pressure
d	i.d. of tube
f	friction factor for homogeneous flow
G	mass velocity
h_{FC}	forced convection heat transfer coefficient
H_{fg}	latent heat of evaporation
i_L	local liquid enthalpy (function of T_L)
i_{sat}	enthalpy of saturated liquid
k	vapor velocity coefficient
L_B	length of vapor blanket
Pr_L	Prandtl number of liquid, $\mu_L c_{pL}/\lambda_L$
q	heat flux
q_c	critical heat flux
q_B	fraction of q for boiling
Re	Reynolds number for homogeneous flow, Gd/μ
T_L	local liquid temperature (function of i_L)
T_{sat}	saturation temperature
T_w	wall temperature
U_B	vapor blanket velocity
U_δ	homogeneous flow velocity at distance δ from wall
x	true quality
x_e	local thermodynamic equilibrium quality
$x_{e,N}$	x_e at the incipience of net vapor generation.

Greek symbols

α	void fraction
δ	sublayer thickness
λ_L	thermal conductivity of liquid
μ	viscosity for homogeneous flow
μ_L	viscosity of liquid
μ_v	viscosity of vapor
ρ	density for homogeneous flow
ρ_L	density of liquid
ρ_v	density of vapor
σ	surface tension
τ	vapor blanket passage time
τ_w	wall shear stress of homogeneous flow.

fluids in the range of $\alpha < 0.7$, for which the assumption of homogeneous flow may be tolerated.

However, k evaluated by equation (2) is not continuous in magnitude at the boundary between two adjacent regimes of α, which gives rise to some degree of discontinuity in the predicted value of CHF (see thin lines in Fig. 6, for example). Besides, for the use of equation (2), an averaging procedure of CHF value near the boundary between two adjacent regimes of α is needed (see ref. [2] for details), causing a remarkable increase of computational time. In addition, equation (2) exhibits comparatively low accuracy in predicting CHF for non-aqueous fluids.

Hence, it is desired that the foregoing defects associated with equation (2) should be removed; if this is realized, the foregoing predictive procedure becomes much more useful in various aspects. The present paper reports the results of a study which has been carried out with these objectives.

2. A NEW CORRELATION OF k AND PREDICTION ACCURACY OF CHF

Experimental CHF data of subcooled flow boiling employed in the present study are listed in Table 1, where the number of data points, the ranges of diameter d, pressure p, mass velocity G, subcooling $T_{sat} - T_L$ and thermodynamic equilibrium quality x_e at the CHF location, and the range of vapor/liquid density ratios ρ_v/ρ_L are shown, together with the reference number of each data source.

As already mentioned, the data of ref. [4] for water were employed in the previous paper [2] to derive a rather tentative correlation of k, that is, equation (2). In the present study, all of the 835 points data for the various materials listed in Table 1 have been analyzed to investigate the possibility of deriving a synthetic correlation of k. For this purpose, the magnitude of k is evaluated first through the calculation procedure of the Appendix, so that the CHF value predicted with the magnitude of k may agree with the corresponding experimental data of CHF. In the course of this computation, quantities such as void fraction α, Reynolds number Re, density ratio ρ_v/ρ_L, and others can also be determined relating to each value of k.

For the value of α thus evaluated, it is found that the condition of $\alpha < 0.7$ is satisfied by as many data points as listed in the third column of Table 1. Then, $k \cdot Re^{0.8}$ obtained for each of these data points is plotted against ρ_v/ρ_L in a similar way to the previous study [2], and some typical examples of the results are shown in Figs. 2–5, where Fig. 2 represents the data for $\alpha = 0.55$–0.65, Fig. 3 for $\alpha = 0.35$–0.45, Fig. 4 for $\alpha = 0.05$–0.15, and Fig. 5 for $\alpha = 0$, respectively. In these figures, different fluids are represented by different symbols: ○ for water, + for R-12, × for R-11, ▽ for nitrogen, □ for helium, and △ for R-113.

Then, with the help of least squares and other means, various types of formulae have been tested to correlate the data of k such as those cited above, resulting in the following expression:

$$k = \frac{242[1 + K_1(0.355 - \alpha)]}{[0.0197 + (\rho_v/\rho_L)^{0.733}][1 + 90.3(\rho_v/\rho_L)^{3.68}]} Re^{-0.8} \quad (3)$$

Table 1. Number of data points and experimental conditions for the CHF data analyzed

Fluid	No. of data	Data of $x < 0.7$	d (mm)	p (MPa)	G (kg m^{-2} s^{-1})	$T_{sat} - T_L$ (K)	$-x_e$	ρ_v/ρ_l	Ref.
Water	374	307	8	2.9–19.6	500–5000	0–75	0–0.835	0.018–0.321	[4]
Water	270†	270	7.72–11.07	3.4–13.8	350–10 360	1.8–97.6	0.010–0.493	0.021–0.136	[5]
R-12	53‡	53	5	1.9–3.4	770–5400	0.0–10.4	0.004–0.264	0.108–0.311	[6,7]
R-11	37	37	12.47	1.0–2.5	1390–8800	18.3–61.3	0.155–0.619	0.046–0.139	[8]
Nitrogen	51	51	12.80	0.5–1.7	550–2260	3.0–26.2	0.042–0.477	0.030–0.118	[9]
Helium	11	11	1	0.199	35–90	0.0–0.159	0.021–0.191	0.410	[10]
Helium	4	4	1.09	0.194–0.199	79–104	0.0–0.198	0.034–0.216	0.381–0.410	[11]
R-113	35	35	10.2	0.9–2.2	1280–5600	0.47–30.8	0.005–0.544	0.050–0.167	[12]
Total	835	768	1.0–12.8	0.199–19.6	35–10 360	0–97.6	0.835	0.018–0.410	—

† Nine clearly abnormal data points have been omitted from the original data.
‡ Data points of $\Delta p/p > 0.03$ have been omitted from the original data (see ref. [2] for details).

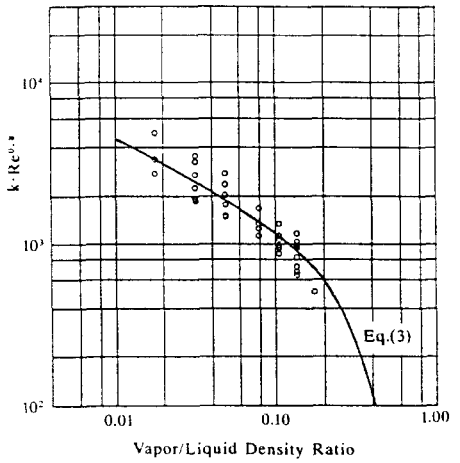

FIG. 2. Velocity coefficient (void fraction: $0.55 < x < 0.65$).

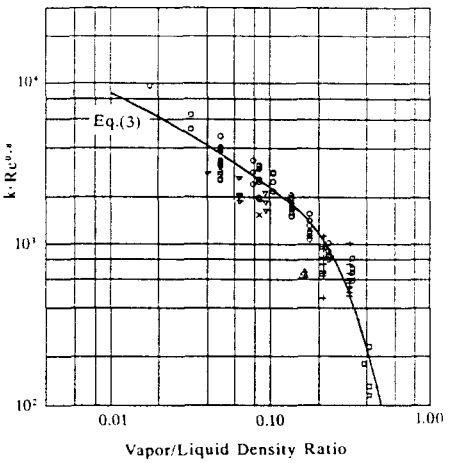

FIG. 4. Velocity coefficient (void fraction: $0.05 < x < 0.10$).

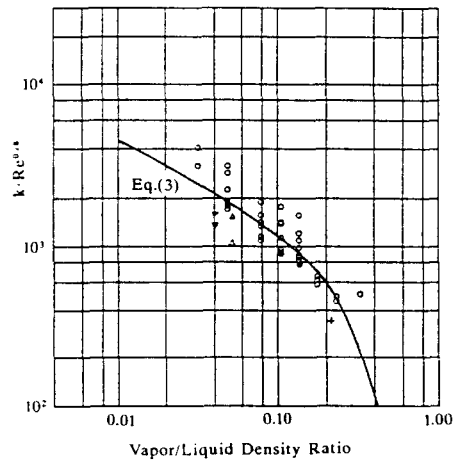

FIG. 3. Velocity coefficient (void fraction: $0.35 < x < 0.45$).

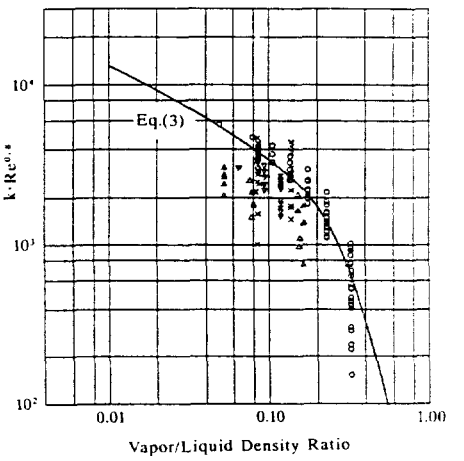

FIG. 5. Velocity coefficient (void fraction: $x = 0$).

Table 2. Prediction accuracy for CHF of various fluids

Fluid	Data of $x < 0.7$	k of equation (2) $\mu(R)$	k of equation (2) $\sigma(R)$	k of equation (3) $\mu(R)$	k of equation (3) $\sigma(R)$	Ref.
Water	307	1.030	0.167	0.978	0.144	[4]
Water	270	1.085	0.192	1.021	0.120	[5]
R-12	53	1.159	0.247	1.064	0.291	[6, 7]
R-11	37	1.182	0.247	1.039	0.271	[8]
Nitrogen	51	1.337	0.215	1.165	0.145	[9]
Helium	11	1.614	0.294	1.038	0.179	[10]
Helium	4	1.641	0.337	1.147	0.260	[11]
R-113	35	1.632	0.411	1.494	0.387	[12]
Total	768	1.125	0.260	1.040	0.210	—

where $K_1 = 0$ for $x > 0.355$, and $K_1 = 3.76$ for $x < 0.355$. Respective lines in Figs. 2–5 represent equation (3) with $x = 0.6$ in Fig. 2, $x = 0.4$ in Fig. 3, $x = 0.1$ in Fig. 4, and $x = 0$ in Fig. 5, indicating that, in spite of its simple form, equation (3) is capable of correlating k fairly well over a wide range of conditions.

Now, as for the accuracy of predicting CHF in the range of $x < 0.7$, the procedure of the previous paper [2] employing equation (2) is compared with that of the present paper employing equation (3) in Table 2, where R is defined as

$$R = (\text{predicted CHF})/(\text{measured CHF})$$

and $\mu(R)$ and $\sigma(R)$ are the mean value and standard deviation of R, respectively. In this statistical computation of prediction accuracy, nine data points of water for $p = 19.6$ MPa and $T_{sat} - T_L = 0$ K, included in the U.S.S.R. CHF table [4], have been omitted because they exhibit rather regular deviation as compared with all the other data. In any case, the results of Table 2 indicate that equation (3) is capable of predicting CHF with comparatively good accuracy for various fluids except for the data for R-113 of Coffield *et al.* [12].

Regarding the exceptional character of the R-113 data mentioned above, it may be of use to point out that nitrogen gas was used to pressurize the fluid in the loop of Coffield *et al.* [12]. In other words, a noticeable gas volume (the volume in the pressurizer plus that of the gas bomb) was attached to the loop on the entrance side of the test tube, and there might have been a certain measure of flow pulsation to lower the magnitude of the CHF.

3. IMPROVEMENT OF CHF PREDICTION ACCURACY FOR WATER

From the results obtained in the preceding section, it is clear that the use of equation (3) is superior to that of equation (2) with respect to the prediction accuracy; besides, the use of equation (3) instead of equation (2) can remove defects such as the discontinuity in the predicted CHF value and the increase of computational time.

Nevertheless, the accurate prediction of the CHF for water is particularly important in technology, and accordingly, more detailed analyses of k for water will be mentioned below. If the 307 data points of water listed in the first line of Table 2 are divided into eight subregions of x, they give the results of Table 3 for prediction accuracy. Similarly, 270 data points of water in the second line of Table 2 give the results shown in Table 4. These two tables disclose that the CHF prediction based on equation (3) exhibits somewhat lower accuracy in the regime of $x < 0.1$ as compared with the regime of $x > 0.1$.

If one wants to improve the prediction accuracy for $x < 0.1$, it can be done in the following way: a simple correction term is included on the right-hand side of equation (3) to give:

$$k = \frac{242[1 + K_1(0.355 - x)][1 + K_2(0.100 - x)]}{[0.0197 + (\rho_v/\rho_L)^{0.733}][1 + 90.3(\rho_v/\rho_L)^{3.68}]} Re^{-0.8} \tag{4}$$

where K_1 is the same as in equation (3), while $K_2 = 0$ for $x > 0.100$ and $K_2 = 2.62$ for $x < 0.100$. The accuracies of CHF prediction with equation (4) are also listed in Tables 3 and 4, indicating that, in the case of water including the regime $x < 0.1$, the use of equation (4) is preferable.

4. ADDITIONAL REMARKS

4.1. *Variation of CHF with diameter*

Figure 6 represents the variation of critical heat flux q_c with diameter d: thin and thick lines are the results of predictions of CHF for water at $p = 13.79$ MPa, $G = 2065$ kg m^{-2} s^{-1}, and $T_{sat} - T_L = 26$ K ($x_e = -0.146$), while three open circles represent the experimental data of water collected from ref. [5] for nearly the same conditions of p, G, and $T_{sat} - T_L$ as above.

In Fig. 6, thin lines represent the CHF value pre-

Table 3. Prediction accuracy for water CHF data of ref. [4]

Range of x	Data points	k of equation (2)		k of equation (3)		k of equation (4)	
		$\mu(R)$	$\sigma(R)$	$\mu(R)$	$\sigma(R)$	$\mu(R)$	$\sigma(R)$
0.6–0.7	28	1.164	0.203	1.034	0.191	1.034	0.191
0.5–0.6	30	1.079	0.261	1.006	0.224	1.006	0.224
0.4–0.5	28	1.093	0.167	1.014	0.173	1.014	0.173
0.3–0.4	31	1.036	0.141	1.009	0.116	1.010	0.114
0.2–0.3	37	1.090	0.110	1.028	0.102	1.028	0.102
0.1–0.2	36	1.037	0.108	0.997	0.094	1.005	0.082
0–0.1	55	0.934	0.113	0.927	0.095	1.008	0.076
0	62	0.958	0.112	0.911	0.103	1.001	0.098
Total	307	1.030	0.167	0.978	0.144	1.012	0.132

Table 4. Prediction accuracy for water CHF data of ref. [4]

Range of x	Data points	k of equation (2)		k of equation (3)		k of equation (4)	
		$\mu(R)$	$\sigma(R)$	$\mu(R)$	$\sigma(R)$	$\mu(R)$	$\sigma(R)$
0.6–0.7	4	0.810	0.059	0.891	0.064	0.891	0.064
0.5–0.6	6	0.883	0.147	0.976	0.159	0.976	0.159
0.4–0.5	7	1.011	0.217	0.958	0.157	0.958	0.157
0.3–0.4	32	1.128	0.163	1.026	0.075	1.026	0.075
0.2–0.3	57	1.119	0.192	1.085	0.104	1.085	0.104
0.1–0.2	77	1.152	0.204	1.076	0.129	1.077	0.129
0–0.1	69	0.988	0.147	0.960	0.063	1.040	0.048
0	18	1.136	0.052	0.879	0.041	1.000	0.047
Total	270	1.085	0.192	1.021	0.120	1.050	0.105

dicted by the method of the previous paper [2] employing k of equation (2), while a continuous thick line represents the result of the present work with k of equation (4), showing that the latter method can predict the magnitude of CHF in a continuous form. For reference, the variation of void fraction α accompanying the continuous change of CHF in Fig. 6 is represented in Fig. 7, where sharp bends can be seen at A and B where $\alpha = 0.355$, and at C where $\alpha = 0.100$. However, this is only a superficial matter resulting from an empirical form of equation (4) (primarily, the curve must be smooth at these points). An important observation in Fig. 7 is the fact that even if p, G, and $T_{sat} - T_L$ are fixed, the magnitude of α at the CHF condition changes with d, and besides, has a peak value on the way.

4.2. *Comparison of predicted and measured CHF*

The accuracy of the CHF prediction procedure employing either equation (3) or equation (4) has already been discussed based on $\mu(R)$ and $\sigma(R)$ in Tables 2–4. However, visual comparisons between the

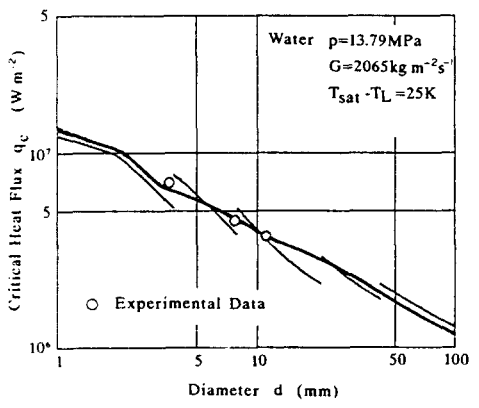

FIG. 6. Variation of critical heat flux with tube diameter.

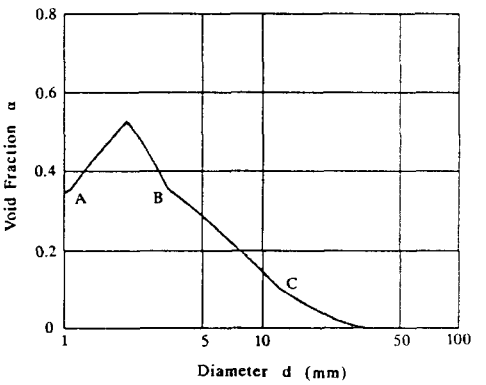

FIG. 7. Variation of void fraction at CHF condition corresponding to the state of Fig. 6.

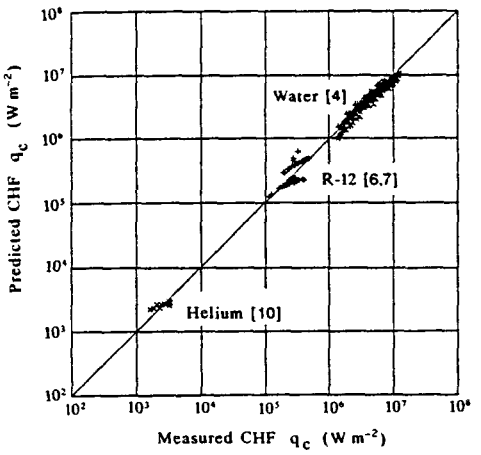

FIG. 8. Comparison of predicted and measured critical heat flux.

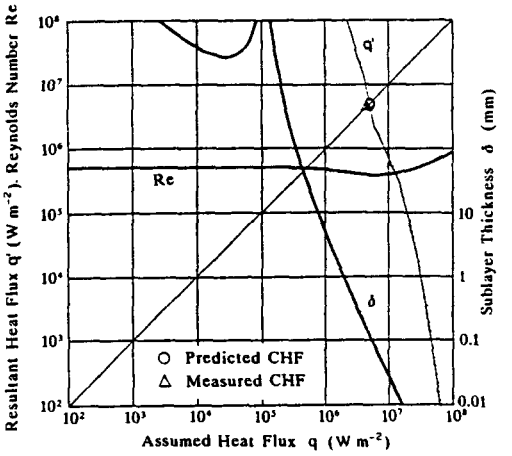

FIG. 10. Relationship between assumed q and resultant q', Re, and δ.

predicted and the measured values of CHF are also of use, so they are shown in Figs. 8 and 9. In these figures, the predicted values for water have been computed with k of equation (4), while those for non-aqueous fluids have been predicted with k of equation (3).

4.3. *A note on the root of* $q = q'$

The prediction procedure of CHF summarized in the Appendix begins its calculation by assuming a value of the heat flux q, and finally a resultant value of the heat flux q' is derived. Hence, if the magnitude of q undergoes a change, it gives q' which varies as a function of q. A typical example of the relationship between q and q' thus obtained is shown in Fig. 10 for the case of water at $p = 11.8$ MPa, $G = 5000$ kg m^{-2} s^{-1}, and $T_{sat} - T_L = 0$ K, where the foregoing function $q' = f(q)$ is represented by a thin line: clearly, the magnitude of CHF is predicted at the location of O where $q = q'$, while the measured value of CHF is located at △. For reference, the accompanying variations of Reynolds number Re and the sublayer thickness δ are also represented by thick lines in Fig. 10.

Usually, the relationship between q and q' takes the form shown in Fig. 10, so no problems arise in predicting CHF by iterative procedures. However, in the case of very high magnitudes of pressure and subcooling (actually, water at $\rho_v/\rho_L = 0.321$ and $T_{sat} - T_L = 50$–75 K in the present study), the situation of Fig. 10 is transformed into a special form (Fig. 12) passing through an intermediate one (Fig. 11). In a special case such as that shown in Fig. 12, four roots of $q = q'$ exist, but a continuous connection with the situation of Fig. 10 must be maintained to predict the value of CHF and accordingly it is found that, among four roots, only one root of the highest value at the location indicated by O can have a physical meaning, and this agrees with the trend of experimental data.

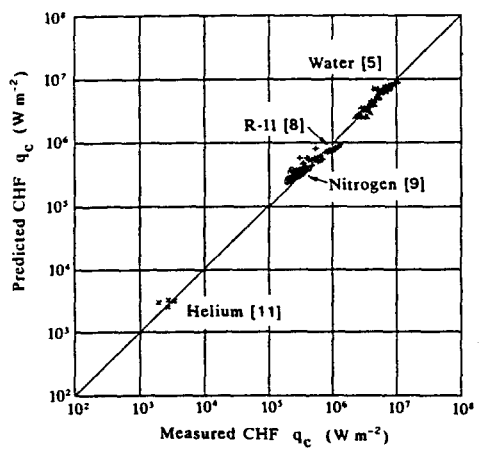

FIG. 9. Comparison of predicted and measured critical heat flux.

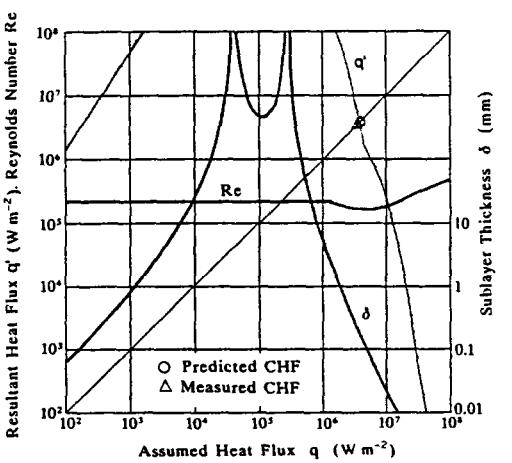

FIG. 11. Relationship between assumed q and resultant q', Re, and δ.

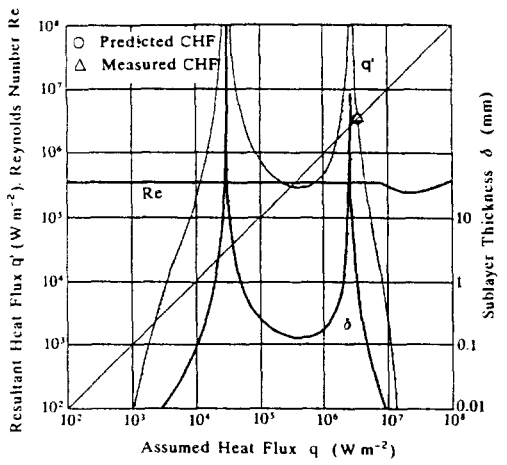

FIG. 12. Relationship between assumed q and resultant q', Re, and δ.

5. CONCLUSIONS

(1) A total of 835 data points of CHF for six kinds of fluids (water, R-12, R-11, nitrogen, helium, and R-113) have been analyzed to investigate the nature of an empirical coefficient (the velocity coefficient) k, which has been introduced in a previous paper in order to establish a physical model for CHF of subcooled flow boiling. Equation (3) has been derived as a new correlation of k.

(2) The foregoing model of CHF is one which is based on the liquid sublayer dryout mechanism, and it is of interest to learn that the velocity coefficient k, which links the vapor blanket velocity with the two-phase flow velocity in a tube, can be correlated in terms of dimensionless groups dominating the two-phase flow; that is, void fraction α, vapor/liquid density ratio ρ_v/ρ_L, and Reynolds number Re.

(3) Employing k of equation (3) [or that of equation (4) to improve prediction accuracy in the regime of $\alpha < 0.1$ for water], the CHF prediction procedure summarized in the Appendix offers a generalized method capable of predicting CHF of subcooled flow boiling with sufficient accuracy up to high degrees of subcooling.

REFERENCES

1. C. H. Lee and I. Mudawar, A mechanistic critical heat flux model for subcooled flow boiling based on local bulk flow conditions, *Int. J. Multiphase Flow* **14**, 711–728 (1988).
2. Y. Katto, A physical approach to critical heat flux of subcooled flow boiling in round tubes, *Int. J. Heat Mass Transfer* **33**, 611–620 (1990).
3. Y. Haramura and Y. Katto, A new hydrodynamic model of critical heat flux, applicable widely to both pool and forced convection boiling on submerged bodies in saturated liquids, *Int. J. Heat Mass Transfer* **26**, 389–399 (1983).
4. Heat Mass Transfer Section, Scientific Council, Academy of Sciences, U.S.S.R., Tabular data for calculating burnout when boiling water in uniformly heated round tubes, *Thermal Engng* **23**(9), 77–79 (1972).
5. B. Thompson and R. V. Macbeth, Boiling water heat transfer burnout in uniformly heated round tubes: a compilation of world data with accurate correlations, U.K.A.E.A., AEEW-R356 (1964).
6. Y. Katto and S. Yokoya, CHF of forced convection boiling in uniformly heated vertical tubes: experimental study of HP-regime by the use of refrigerant 12, *Int. J. Multiphase Flow* **8**, 165–181 (1982).
7. Y. Katto and S. Ashida, CHF in high-pressure regime for forced convection boiling in uniformly heated vertical tubes of low length-to-diameter ratio, *Proc. 7th Int. Heat Transfer Conf.*, Vol. 4, pp. 291–296 (1982).
8. J. C. Purcupile, L. S. Tong and S. W. Gouse, Jr., Refrigerant–water scaling of critical heat flux in round tubes—subcooled forced-convection boiling, *Trans. ASME*, Ser. C, *J. Heat Transfer* **95**, 279–281 (1973).
9. S. S. Papell, R. J. Simoneau and D. D. Brown, Buoyancy effects on critical heat flux of forced convective boiling in vertical flow, NASA, TN D-3672 (1966).
10. Y. Katto and S. Yokoya, Critical heat flux of liquid helium (I) in forced convective boiling, *Int. J. Multiphase Flow* **10**, 401–413 (1984).
11. H. Ogata and S. Sato, Critical heat flux for two-phase flow of helium I, *Cryogenics* **13**, 610–611 (1976).
12. R. D. Coffield, Jr., W. H. Rohrer, Jr. and L. S. Tong, A subcooled DNB investigation of Freon-113 and its similarity to subcooled water DNB data, *Nucl. Engng Des.* **11**, 143–153 (1969).

APPENDIX. CHF PREDICTION PROCEDURE

Assume a value for q under local bulk conditions of p, G, $T_{sat}-T_L$, and d.

Calculation of δ

$$\delta = \frac{\pi(0.0584)^2}{2}\left(\frac{\rho_v}{\rho_L}\right)^{0.4}\left(1+\frac{\rho_v}{\rho_L}\right)\frac{\sigma}{\rho_v}\left(\frac{\rho_v H_{fg}}{q_B}\right)^2$$

where $q_B = q - h_{FC}(T_w - T_L)$, for which

$$h_{FC} = 0.023(Gd/\mu_L)^{0.8}\, Pr_L^{0.4}\,(\lambda_L/d)$$

$$T_w - T_L = \frac{(\Psi_0 - 1)(T_{sat}-T_L) + (q/h_{FC})}{\Psi_0}$$

$$\Psi_0 = 230(q/GH_{fg})^{0.5}.$$

Calculation of x_e and $x_{e,N}$

$$x_e = \frac{i_L - i_{sat}}{H_{fg}}$$

$$x_{e,N} = \begin{cases} -0.0022\dfrac{q}{\rho_L H_{fg}}\dfrac{d}{(\lambda_L/c_{pL}\rho_L)} & \text{for } \dfrac{Gc_{pL}d}{\lambda_L} < 70\,000 \\ -154\dfrac{q}{\rho_L H_{fg}}\dfrac{1}{(G/\rho_L)} & \text{for } \dfrac{Gc_{pL}d}{\lambda_L} > 70\,000. \end{cases}$$

Calculation of x

$$x = \begin{cases} \dfrac{x_e - x_{e,N}\exp\left(\dfrac{x_e}{x_{e,N}} - 1\right)}{1 - x_{e,N}\exp\left(\dfrac{x_e}{x_{e,N}} - 1\right)} & \text{for } x_{e,N} < x_e \\ 0 & \text{for } x_{e,N} > x_e. \end{cases}$$

Calculation of ρ, α, and μ

$$\rho = 1/[x/\rho_v + (1-x)/\rho_L]$$

$$\alpha = x/[x + (1-x)(\rho_v/\rho_L)]$$

$$\mu = \mu_v\alpha + \mu_L(1-\alpha)(1+2.5\alpha).$$

Calculation of U_δ

$$U_\delta^+ = \begin{cases} y_\delta^+ & \text{for } 0 < y_\delta^+ < 5 \\ 5.0 + 5.0 \ln (y_\delta^+/5) & \text{for } 5 < y_\delta^+ < 30 \\ 5.5 + 2.5 \ln y_\delta^+ & \text{for } 30 < y_\delta^+ \end{cases}$$

where $U_\delta^+ = U_\delta/\sqrt{(\tau_w/\rho)}$ and $y_\delta^+ = \delta\sqrt{(\tau_w/\rho)}/(\mu/\rho)$, for which

$$\tau_w = f \cdot \rho(G/\rho)^2/8$$

$$1/\sqrt{f} = 2.0 \log_{10} (Re\sqrt{f}) - 0.8$$

$$Re = Gd/\mu.$$

Calculation of U_B

$$U_B = kU_\delta$$

where k is the velocity coefficient.

Calculation of L_B

$$L_B = 2\pi\sigma(\rho_v + \rho_L)/(\rho_v \rho_L U_B^2).$$

Calculation of q'

$$q' = \delta\rho_L H_{fg}/\tau$$

where $\tau = L_B/U_B$; q is the critical heat flux q_c when $q = q'$

PREDICTION DU FLUX THERMIQUE CRITIQUE D'EBULLITION POUR L'ECOULEMENT SOUS-REFROIDI DANS DES TUBES CIRCULAIRES

Résumé—Basé sur le mécanisme d'assèchement de la sous-couche liquide, un modèle physique du flux thermique critique (CHF) d'ébullition d'un liquide sous-refroidi en écoulement a été présenté antérieurement avec une formule de coefficient k pour lier la vitesse d'une couverture de vapeur à celle de l'écoulement diphasique. On présente ici une nouvelle formule de ce coefficient de vitesse k qui est obtenu à partir des données de CHF pour différentes sortes de fluides, ce qui permet de prédire de façon générale le CHF d'ébullition avec convection dans le domaine de sous-refroidissement $T_{sat} - T_L \geqslant 0$ K, de fraction de vide $\alpha < 0{,}7$, et de rapport de masse volumique vapeur/liquide $\rho_v/\rho_L > 0{,}01$. Des comparaisons entre CHF mesurés et calculés montrent une bonne précision jusqu'à de forts degrés de sous-refroidissement.

BERECHNUNG DER KRITISCHEN WÄRMESTROMDICHTE BEIM UNTERKÜHLTEN STRÖMUNGSSIEDEN IN KREISROHREN

Zusammenfassung—In einer früheren Arbeit wurde ein physikalisches Modell für die kritische Wärmestromdichte (CHF) beim unterkühlten Strömungssieden vorgestellt, das auf dem Dryout-Mechanismus der Flüssigkeitsunterschicht basiert. Dieses Modell enthält eine eher tastende Korrelation für den Koeffizienten k, welcher die Geschwindigkeit der Dampfbedeckung mit der Geschwindigkeit der Zweiphasenströmung verbindet. In dieser Arbeit wird nun eine neue Korrelation für den Geschwindigkeitskoeffizienten k ermittelt, die sich auf die CHF-Daten verschiedener Fluidarten stützt. Es wird eine allgemeine Methode zur Berechnung der kritischen Wärmestromdichte beim unterkühlten Strömungssieden für eine Unterkühlung $T_{sat} - T_L \geqslant 0$ K, einen Dampfgehalt $\alpha < 0{,}7$ und ein Dampf/Flüssigkeits-Dichteverhältnis $\rho_v/\rho_L > 0{,}01$ vorgestellt. Die berechneten und gemessenen kritischen Wärmestromdichten stimmen bis zu großen Unterkühlungen ziemlich gut überein.

ОПРЕДЕЛЕНИЕ КРИТИЧЕСКОГО ТЕПЛОВОГО ПОТОКА ПРИ ТЕЧЕНИИ НЕДОГРЕТОЙ ЖИДКОСТИ В КРУГЛЫХ ТРУБАХ

Аннотация—В предыдущей статье на основе механизма кризиса теплообмена в жидком подслое разработана физическая модель критического теплового потока (КТП) при течении недогретой жидкости в условиях кипения, а также получена приближенная зависимость для коэффициента k, связывающая скорость паровой рубашки и двухфазного потока. В предлагаемой статье на основе данных по КТП при различных видах течения выведена новая зависимость для коэффициента k, представляющая собой обобщенный метод расчета КТП при течении недогретой жидкости в условиях кипения в диапазоне недогрева $T_{sat} - T_L \geqslant 0$ К, для объемного содержания $\alpha < 0{,}7$ и соотношения плотностей пара и жидкости $\rho_v/\rho_L > 0{,}01$. Сравнение расчетных и измеренных КТП показало удовлетворительное согласие даже при высоких уровнях недогрева.